Journal of Integrative Neuroscience, Vol. 8, No. 3 (2009) 323–344

Imperial College Press
www.icpress.co.uk

Research Report

ON THE ORGANIZATION OF RECEPTIVE FIELDS OF ORIENTATION-SELECTIVE UNITS RECORDED IN THE FISH TECTUM

ILIJA DAMJANOVIĆ*, ELENA MAXIMOVA and VADIM MAXIMOV

Institute for Information Transmission Problems
Russian Academy of Sciences
Bolshoi Karetny 19, 127994 Moscow, Russia
**damjanov@iitp.ru*

Received 7 August 2009
Accepted 17 August 2009

Responses from two types of orientation-selective units of retinal origin (detectors of horizontal lines and detectors of vertical lines) were recorded extracellularly from their axon terminals in the medial sublamina of tectal retinorecipient layer of immobilized cyprinid fish *Carassius gibelio*. Excitatory and inhibitory influences across receptive fields of orientation-selective units were evaluated. Positions, sizes and forms of the responsive parts of the receptive field were estimated by moving edges and flashing narrow light and dark stripes. It was shown that the orientation-selective units in fish are characterized by small responsive receptive fields with mean width of $4.8 \pm 1.6^\circ$ ($n = 176$). The comparison of different types of orientation-selective units revealed that the responsive receptive fields of detectors of vertical lines are significantly wider (13%) than those of detectors of horizontal lines. Statistically significant difference was also found between sizes of responsive receptive fields evaluated by light and dark edges. Mean responsive receptive field width, estimated for light edges (ON responses) were wider than those evaluated for dark edges (OFF responses). Inhibition in the receptive field of orientation-selective units was evaluated on the basis of two experimental methods. Evidence that signals are not linearly summed across the receptive field was derived from experimental results. Inhibitory influences, recorded in the receptive field of orientation-selective units, always initiated inside the responsive receptive field area and spread towards the periphery. Results of the study indicate that receptive fields cannot be defined as homogeneous sensory zone driven by a linear mechanism of response generation. The receptive fields of orientation-selective units, in fish appear to be composed of subunits sensitive to the appropriately oriented stimuli.

Keywords: Tectum opticum; *Carassius gibelio*; orientation selectivity; receptive field; inhibitory surround.

1. Introduction

Visual information is first processed in the retina of vertebrates. Specialized ganglion cells (detectors) are selectively tuned to detect various features of the visual scene,

*Corresponding author.

including direction and speed of motion, form, color and size of the stimuli. Information processed at the retinal level of lower vertebrates by different types of detectors is transmitted to different primary visual centers of the brain; one in particular is the midbrain formation, tectum opticum (TO). Axons of different detectors terminate in different tectal levels in frogs [23] and fish [18]. Retinotectal projections were investigated in different cyprinidae [18,20,28–32], pike [41], trout [25] and several other sea fish species [33]. In comparison to more primitive frog visual system, where five different retinal detectors were described [23], more than a dozen different detectors of retinal origin were recorded in the fish TO [28,29]. Axons of direction-selective units terminate in the superficial sublamina of the TO retinorecipient layer [7]. Projections of orientation-selective units (OSUs), spot detectors and color-opponent units terminate below the sublamina of direction-selective units. Units characterized by sustained responses to dark or light stimuli project to the deepest sublaminae of the tectal retinorecipient layer.

In the fish, two types of OSUs sensitive to movement of horizontal and vertical lines in directions orthogonal to the orientation of line were observed: detectors of horizontal lines supposedly of retinal origin were recorded first in the TO of pike [41] and several marine fish [33], while detectors of vertical lines (besides the detectors of horizontal lines) were recorded in the *Carassius carassius* [32]. It was shown that both types of OSUs project to the medial sublamina of the tectal retinorecipient layer. The classification of OSUs in retinotectal projection of cyprinid fish *Carassius gibelio* (Bloch, 1782) was carried out and their properties were thoroughly investigated in a recent study [30]. The OSUs of the fish retinotectal system were proved to divide into two types according to their preferred orientation (approximately horizontal or vertical). These types practically do not differ from each other except for preferred orientation. Both of them were ON–OFF type, as distinct from the direction-selective units, which are represented by separate ON and OFF cell subtypes [28, 29]. The OSUs were so symmetrical in all their properties (besides the preferred orientation) that it was difficult to differentiate a detector of horizontal lines from a detector of vertical lines, unless orientation of the applied stimulus was known *a priori* [32]. Similarly, by just looking at the cell responses it was difficult to differentiate what sign of contrast the applied stimulus had.

Polar diagrams of the OSUs were measured with contrast edges moving across the receptive field (RF) in different directions. Polar diagrams for both types of OSUs had a figure-eight shape with various opening angles. In comparison with other retinal detectors, the OSUs (along with the direction-selective units) possess the finest spatial resolution. It was shown that OSUs have rather high contrast sensitivity that does not depend on the type of stimulation. Like the direction-selective units, the OSUs respond to contrast edges differing in their brightness from the background by 3–5% only [30].

The OSUs of retinal origin were also described in birds [26], turtle [5] and mammals [2–4, 12, 24]. It is known that many cells from the mammalian visual

cortex are orientation selective. Such units were recorded in primary visual cortex of different mammal species [10, 14, 17, 19, 34]. According to organization of their RFs these units were classified as simple, complex and hypercomplex cells (see Ref. 13 for a review). The RF of a simple cell is characterized by a narrow region of excitation, flanked on both sides by larger peripheral regions of inhibition. Complex cells are assumed to be constructed from simple ones. Complex cells, just like simple cells, respond over a limited region of the visual field to properly oriented slits, bars, or edges regardless of where the stimulus is placed in the RF. However, unlike simple cells, their behavior cannot be explained by a distinct subdivision of the RF into excitatory and inhibitory regions. Both simple and complex cells usually show length summation: the longer the stimulus line, the better the response is, until the line is as long as the RF. After that the response remains constant and longer stimuli produce no increase of the response. On the other hand, in hypercomplex (end-stopped) cells, lengthening the line improves the response up to a limit, but exceeding that limit in one or both directions results in weaker response.

The RF structure of fish retinal OSUs were investigated in the electrophysiological study of retinotectal projections in *C. carassius* with the use of stimuli moved manually or mechanically [31, 32]. Experiments were directed primarily at investigation of interaction of signals within the RF by using simultaneously presented edges and lines of mutually-orthogonal orientations, or by using stimuli of different lengths. It was shown that lengthening the adequately oriented stimuli out of RF area did not affect OSU responses. No studies of the interaction of stimuli in transversal direction were carried out. Therefore flanking inhibitory regions were not detected in the RF. On that basis, Maximova and Maximov [32] concluded that RF structure of the fish OSUs is similar to the structure of RFs described in mammalian cortical complex cells [15, 35]. The aim of the present study is to evaluate more precisely the excitatory and inhibitory influences underlying signal interaction within the OSU RF. The main focus will be on the organization of the RF in the transverse direction (relative to the preferred orientation), including identification and localization of the inhibitory surrounds, and the investigation of the nature of lateral interaction of signals. This makes the task essentially one-dimensional. Central area of the cell RF, from which responses can be elicited by visual stimulation, will be referred as responsive receptive field (RRF) hereafter [27].

2. Materials and Methods

2.1. *Experimental animals*

The data were collected from several *Carassius gibelio* (Bloch, 1782), which varies between 10 and 15 cm in length and weigh 35 to 100 g each. The fish were acquired from local suppliers (Moscow region) and maintained for several months in aerated fresh water aquaria at room temperature (18–22°C) and natural daylight regime.

2.2. *Preparation*

During the experiments the animals were immobilized (d-tubocurarine, *i.m.*). The dosage of tubocurarine (0.3 mg/100 g) was adjusted to induce immobilization of eyes and respiratory movements. The fish were placed in their natural position in a transparent Plexiglas tank where artificial respiration was provided continuously by forcing aerated water through their gills. In order to reveal the TO contralateral to the stimulated eye, an opening was made in the skull over the contralateral midbrain. During surgery the preparation site of the head was anesthetized with ice. The dura and pia mater were dissected and excess of fatty tissue and fluid were aspirated. The water level in experimental tank was kept constant, while the fish eyes were kept under water. The animals were decapitated after the experiment, and their brain and eyes were used for histological explorations.

2.3. *Visual stimulation*

Visual stimuli (moving contrast edges and light or dark stationary stripes on a gray background) were presented on the computer-controlled 17″ CRT monitor to the right eye of the fish through the transparent tank wall. The stimulation area exceeded the RFs of the investigated units in sizes and was a square with side of approximately 11° on the monitor screen (as a whole, occupying 45° × 35° of the fish visual field). During the experiment, the stimulation area was located on the appropriate place of the monitor screen to cover the RF of the cell under study. Constant luminosity was maintained for the rest of the monitor screen. The distance between the monitor screen and the fish was about 30 cm. When calculating the angular size of the stimuli, the refraction of the rays on the front wall of the aquarium was taken into account.

The visual stimuli used are of two types: moving edges and stationary stripes. The "edge stimuli" are wide light or dark stripes exceeding stimulation area in width. Cell responses were recorded during the stimulus movement across the stimulation area. In this case, at first the leading edge of the stimulus gradually went across the RF of the unit, and after some delay the trailing edge crossed the RF. Orientation of stimuli could be varied. An example of responses of a detector of vertical line to such a moving dark stimulus of preferred orientation is shown in Fig. 1(a). One can see that the cell response is characterized by two spike discharges caused by the leading and the trailing edges of the stimulus moving across the RF.

Another type of stimuli is adequately oriented stationary contrast stripes, flashing at different positions of the stimulation area. These flashing stripes, varying in width from 10′ to 5°30′ in different experiments, are significantly narrower than the stimulation area. A response of the same detector of vertical line to the flashing dark vertical stripe of 10′ in width is shown in Fig. 1(b). When projected to the fish retina, the stripe of this width corresponds approximately to a typical distance between rows of double cones in the *C. gibelio* retina [29]. Responses to the flashing stimulus are characterized by delay of approximately 40 ms. The highest frequency

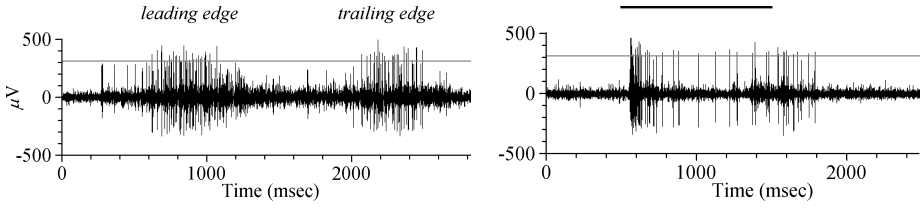

(a) (b)

Fig. 1. Responses of one detector of vertical line to different types of stimuli. (a) Spike discharges of the detector of vertical line evoked by leading and trailing edges of vertical dark "edge stimulus" moving in a caudo-rostral direction at a speed of 11°/sec against a neutral (gray) background. Thin horizontal line represents criterion level used for amplitude discrimination of spikes. (b) Response of the same detector of vertical line to a thin dark vertical stationary stripe (stimulus width 10′), that flashed in the center of the RRF against a neutral (gray) background. Duration of stimulus was 1 sec (marked by horizontal bar at the top panel of the figure).

of spikes in the response is usually recorded during the initial 100–200 ms of stimulation. During subsequent periods of stimulation, frequency of spikes gradually decreases, but is usually not reduced to zero. A significant number of OSUs (90% of cells explored) were shown to respond to stationary stripes of preferred orientations by sustained discharge. Such OSU continue to respond to fixed thin dark or light line within hours [32]. Stimulus switch-off was followed by transient spike discharge that ceased after several hundreds of ms.

2.4. *Data acquisition*

Responses of OSUs were recorded extracellulary in the tectal retinorecipient layer. Low impedance (200–500 KΩ) microelectrodes were made using micropipettes filled with a Wood's metal and tipped with a platinum cap of 2–10 μm in diameter [9]. The microelectrode was guided to a necessary tectal area under visual control by means of a micromanipulator according to the retinotopic projection [18]. Stable single-unit responses from OSUs were regularly recorded in the medial sublamina of tectal retinorecipient layer, beneath the superficial sublayer of direction-selective units. The main criteria characterizing the single-unit response was the high and stable spike amplitude and the high signal/noise ratio. The responses gained in an AC preamplifier (band pass 100 Hz to 3.5 kHz) were listened in a loudspeaker, monitored on an oscilloscope and digitized by an A/D converter (25 kHz sampling rate). Responses, loaded into the computer during the registration interval, were stored as either (a) without any processing (for subsequent analysis of spike form); or (b) after filtering according to amplitude discrimination. They were stored as a sequence of moments of the spike appearance for further processing.

Visual stimulation and data acquisition were guided by independent computer modules. These modules were mutually connected and synchronized in the experimental setup with a third independent computer, which served for on-line graphic

demonstration of processed results (on a separate monitor) and for operative control of stimulation and recording parameters during the experiment. The system of three mutually connected and synchronized computer modules used in the setup are described in detail elsewhere [7, 29].

2.5. *Data processing*

2.5.1. *Polar diagram measurements*

All experimental procedures, performed for investigation of the RF structure, were preceded by measurement of the cell polar diagram and determination of position of the RRF center. An example of polar diagrams for one detector of horizontal line and one detector of vertical line is shown in Figs. 2(a) and 2(b), respectively. Responses to the contrast edges moving in 24 different directions over the neutral (gray) background are presented in the diagrams. Three stimulus trials were usually applied for each direction. Black dots represent a mean number of spikes, calculated over repeated trials for each direction. At the end of the procedure, a measurement of the first direction was repeated in order to check the unit response level. Preferred directions of the stimulus movement perpendicular to its orientation (marked by the arrows in Fig. 2) were determined according to phase of second harmonic of Fourier transform of polar diagram. One can notice that polar diagrams, calculated for leading and trailing edges of the stimuli, were practically symmetrical.

2.5.2. *Determination of the RRF center*

Position of the RRF in the stimulation area was outlined from cell responses to the contrast edge moving in many different directions. The same experimental data, which are used for polar diagram measurements, were applied for determination of the cell RRF center. The RRF center was evaluated from the sequences of moments of spike appearances in all trials for all 24 directions of movement. The automatic procedure that determines the position of the RRF center is as follows. The deviation of the moment of spike appearance from the moment a stimulus passes through the assumed RRF center is calculated for each of the applied directions. The center of the RRF was determined as a point in the visual field, where the mean square deviation calculated for all directions was minimal. As a rule, after the measurement of the polar diagram and determination of the position of the RRF, the position of the area of stimulation on the monitor screen was centered with respect to the RRF, and all subsequent procedures were conducted with the centered RRF. RRFs evaluated in different types of detectors during the perpendicular track of electrode through the tectal retinorecipient layer were shown to be centered in the approximately same position [29, 31].

2.5.3. *Determination of parameters of the box-shaped model of the RRF*

According to the box-shaped model of the RRF, the cell is silent while the stimulus is outside of its RRF and responds by spike discharge only to stimuli placed within

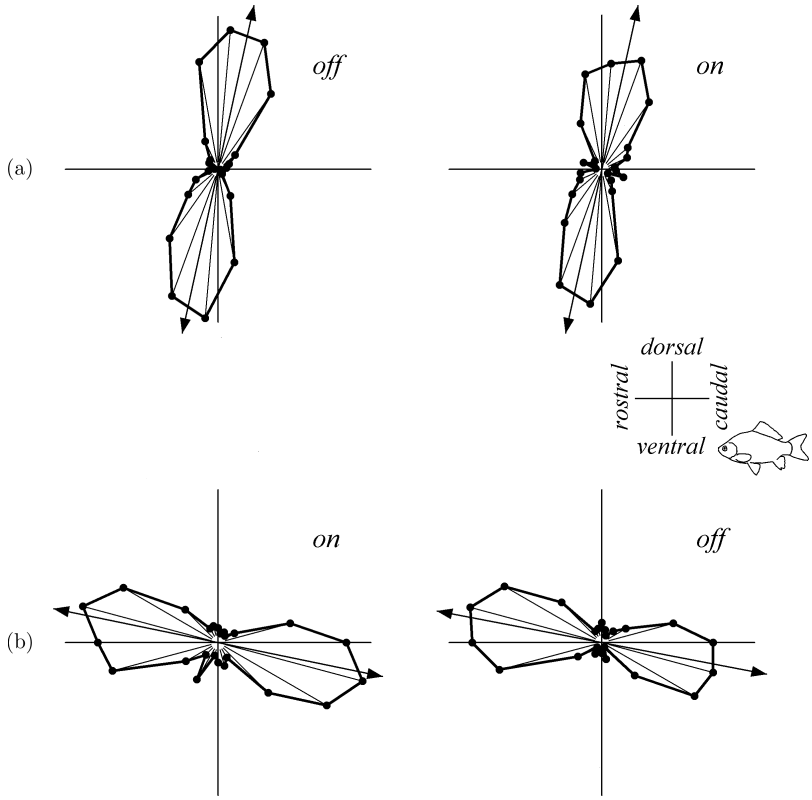

Fig. 2. Examples of polar diagrams of different OSUs. Left and right diagrams correspond to discharges to the leading and the trailing edges, respectively. The coordinate directions in the visual field of the fish are designated in the inset. (a) Polar diagrams of a detector of horizontal line. Responses to dark edges moving in 24 directions at a speed of 16°/sec against a neutral background are presented in the diagram. Dots, joined by the solid line, represent a mean number of spikes in discharges, calculated over repeated trials for each direction. Preferred directions of the cells, determined according to the phase of second harmonic of the Fourier transform, are marked by black arrows. (b) Polar diagrams of a detector of vertical line. Responses to white edges moving in 24 directions at a speed of 16°/sec against a neutral background are presented in the diagram. Display format as in Fig. 2(a).

the RRF. Parameters for the model were determined from experiments with moving edges through the RF. The RRF width along the preferred direction of stimulus movement was evaluated on the basis of the duration of spike discharge, evoked by movement of adequately oriented contrast edges across the stimulation area. Duration of the response was defined as the time interval between the first and the last spike in the discharge. Unfortunately, sparse incidental spikes superimposed on the response can complicate an automatic procedure for such a measurement of the response duration. In order to segregate the evoked spikes from incidental and spontaneous ones generated before and after the evoked train, a special procedure based on the maximum likelihood method was designed. It is proposed that the sequence of spikes in the record was a result of two random processes: the process of high probability (p_d) of spike generation during the discharge, evoked by the

stimulus moving across the cell RRF, and the process with low probability (p_s) of spike generation, reflecting spontaneous activity of the cell before and after the discharge. For this statistical model, a likelihood function (L), which depends on the values of these probabilities and the moments of time, specifying the beginning (t_1) and the end (t_2) of the discharge, is defined:

$$L(p_d, p_s, t_1, t_2) = p_d^{m_d}(1-p_d)^{t_2-t_1-m_d}p_s^{m_s}(1-p_s)^{T-t_2+t_1-m_s}, \tag{2.1}$$

where T is duration of recording in ms, m_d and m_s are functions of t_1 and t_2 and are equal to the numbers of spikes recorded during the discharge (in the interval between t_1 and t_2) and the number of spikes recorded outside of this interval, respectively.

The aim of the procedure was to maximize the function $L(p_d, p_s, t_1, t_2)$ by varying the set of parameters (p_d, p_s, t_1, t_2) and defining moments of the beginning (t_1) and the end (t_2) of the discharge. The difference $t_2 - t_1$ was multiplied by the velocity of the stimulus motion and the result was considered as an estimate of the RRF size for the analyzed unit.

2.5.4. *Determination of parameters of the Gaussian model of the RRF*

According to the Gaussian model of the RRF, the magnitude of the cell response as a function of a stimulus position was approximated by a Gaussian curve. Parameters of the model were determined from (1) post-stimulus histogram of spike discharge, evoked by adequately oriented contrast edge moving across the cell RF, or (2) distribution of spike number across RRF, elicited by appropriately oriented stationary narrow stripes flashing sequentially in different parts of cell RF. Both sets of data were fitted by the Gaussian function with the use of a least-squares minimization algorithm. The equation for Gaussian curve is:

$$G(x) = \frac{N}{\sigma\sqrt{2\pi}}e^{\frac{-(x-\bar{x})^2}{2\sigma^2}}, \tag{2.2}$$

where x is a position of stimulus, $\bar{x}$ is a coordinate of the approximated RRF center, σ is a standard deviation determining Gaussian width and N is a total number of spikes in the discharge. The best Gaussian fit $G(x)$ was considered as an optimal approximation of the cell RRF.

2.5.5. *Determination of parameters of the difference of Gaussians model*

According to a model of the RF, originally proposed by Rodieck and Stone [36], the magnitude of the cell response as a function of a stimulus position is described by a DoG-function ("difference of Gaussians") composed of two terms (excitatory and inhibitory). Applied to the current work, the DoG-function is as follows:

$$D(x) = A_1 e^{-\frac{(x-a_1)^2}{2\sigma_1^2}} - A_2 e^{-\frac{(x-a_2)^2}{2\sigma_2^2}}, \tag{2.3}$$

where x is a position of stimulus, A_1 and A_2 are peak amplitudes of excitatory and inhibitory terms, a_1 and a_2 are positions of centers, and σ_1 and σ_2 are standard deviations determining the widths of excitatory and inhibitory Gaussians, respectively.

One of the experimental methods used to reveal inhibitory influences in OSU RF consisted in stimulation of the unit with two appropriately oriented stationary stripes that flashed simultaneously in different parts of the RF. Experimental data derived by means of this procedure were fitted by the DoG-function. The best DoG fit $D(x)$ was determined by the use of least squares minimization.

3. Results

3.1. *The box-shaped model of the OSU RRF*

In this experimental procedure, the RRF widths of the fish OSUs were estimated on the basis of their responses to adequately oriented contrast edges (horizontal or vertical) moving transversely to its orientation across the cell RF. The results obtained when leading edges of adequately oriented stimuli moved across RF of one detector of horizontal line and one detector of vertical line are shown in Figs. 3(a) and 3(b), respectively. The cell responses were evoked by stimuli moving at speed 11°/sec in ventrodorsal direction, shown in Fig. 3(a), and caudorostral direction, shown in Fig. 3(b). The moments of spike appearance are plotted as dots against the time scales on the top panels. The same data can be considered as positions (x) of stimulus leading edge in the stimulation area at the moment (t) of spike appearance: $x = v \cdot t$, where v is the velocity of edge movement. Corresponding position scales are shown at the bottom of Figs. 3(a) and 3(b). Duration of spike responses shown by dots on the top panels of Figs. 3(a) and 3(b) were estimated by means of maximum likelihood statistical model (2.1). Dashed stepped lines (box-shaped curves) on the bottom panels of Figs. 3(a) and 3(b) represent box-shaped models of the RRFs obtained from the corresponding cell responses.

The RRF widths of OSUs were calculated as a product of duration of spike discharge, evoked by adequately oriented moving stimulus and velocity of the stimulus movement. The RRF sizes were evaluated in $n = 176$ OSUs by means of this procedure. For each unit, the RRF width was estimated for both preferred directions of movement, i.e., for 352 spike discharges. The distribution of RRF widths, estimated for both preferred directions, did not differ significantly from each other. The histogram of RRF sizes distribution, evaluated for both preferred directions in all cells examined, is presented in Fig. 3(c). The RRF widths varied from 1.5° to 11°, with the mean value of 4.8 ± 1.6°. It should be noted that statistically significant difference between mean RRF sizes of detectors of horizontal line and detectors of vertical line was revealed in our study. The RRF widths were estimated for movement of leading edges in both preferred directions in 127 detectors of horizontal lines and in 49 detectors of vertical lines. Mean values for RRF widths of detectors of horizontal lines and detectors of vertical lines amounted to $4.6 \pm 1.6°$ and $5.2 \pm 1.5°$, respectively. The difference in the mean values between the two groups, analyzed by the t-test, was shown to be greater than would be expected by chance; there is a statistically significant difference between the groups ($P = 0.001$).

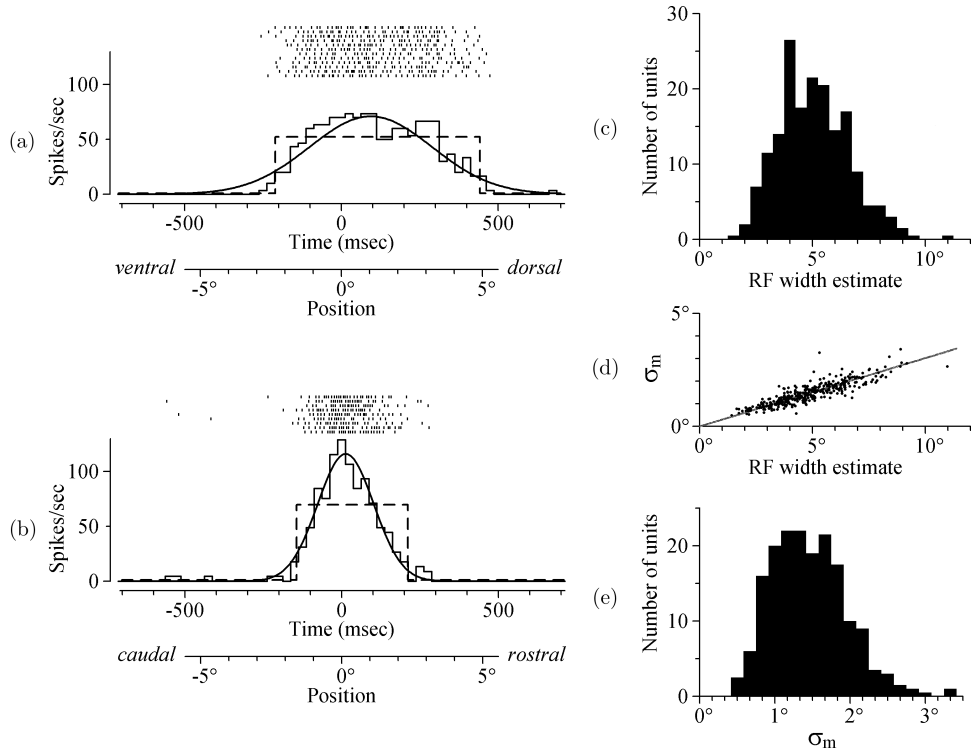

Fig. 3. Determination of the RRF size from the OSU response to contrast edges of preferred orientation, moving in preferred directions across stimulation area. (a) Responses of a detector of horizontal line to dark edges moving across gray background in a ventro-dorsal direction at speed 11°/sec; Top panel: moments of spike appearance during the stimulation, plotted as dots against the time scale, 12 separate rows of dots correspond to different subsequent trials; bottom panel: solid stepped curve is a post-stimulus histogram of the discharge, showing number of evoked spikes along the time or position scales; dashed stepped curve describes the box-shaped model of the discharge according to the maximum likelihood method; solid bell-shaped curve represents Gaussian approximation of the cell response. Time scale: zero point corresponds to the moment when stimulus leading edge passes through the center of stimulation area. Position scale (in angular degrees): zero point corresponds to the position of center of stimulation area; ventro-dorsal direction is positive. (b) Responses of a detector of vertical line to white edges moving across gray background in a caudo-rostral direction at speed 11°/sec. There were 9 subsequent trials in this experiment. Display format as in Fig. 3(a). (c) Histogram of distribution of the RRF sizes estimated by means of maximum likelihood method for 176 OSUs. (d) Scatter plot of the σ-values of the best Gaussian fits for 352 post-stimulus histograms against the RRF widths estimated for the same units by means of maximum likelihood method. (e) Histogram showing distribution of σ-values of the best Gaussian fits for 176 OSUs.

Statistically significant difference was also revealed between the RRF widths evaluated for light and dark edges (the stimuli with different signs of contrast). Mean RRF width, estimated for movement of light leading edges in both preferred directions in $n = 79$ cells (158 responses) was $5.0 \pm 1.5°$, while for movement of dark leading edges (194 responses in $n = 97$ cells) it was $4.6 \pm 1.6°$. The difference in the mean values between the two groups, analyzed by t-test, was shown

to be greater than would be expected by chance; there is a statistically significant difference between the groups ($P = 0.017$).

3.2. *The Gaussian models of the OSU RRF*

3.2.1. *The Gaussian model of the RRF derived from moving edges*

Despite its simplicity, the procedure used in the previous section is self-reliant and performs well at the task of determining the beginning and the end of discharges. A test of this procedure on real experimental data has shown that it successfully eliminates all those spikes which appear occasionally from the standpoint of the experimenter and are not related to the discharge in response to the presentation of the stimulus. Nevertheless, as one can see from Figs. 3(a) and 3(b), the box-shaped curves used for estimation of the RRF width cannot be considered as an optimal approximation of the form of the OSU RRFs — see post-stimulus histograms represented by solid step curves at bottom panels. The post-stimulus histogram, showing the number of evoked spikes along the time and position scales, is usually approximated by Gaussian profiles [8]. Solid bell-shaped curves at the bottom panels in Figs. 3(a) and 3(b) illustrate the least squares fits by Gaussian curves for the corresponding post-stimulus histograms. In the case of such examination a standard deviation value of the Gaussian approximation can be considered as another measure of the RRF width.

In the framework of the Gaussian model of the RRF, the standard deviation values were obtained from the same set of data for 176 OSUs analyzed by the box-shaped model. The σ-values were estimated for both preferred directions, i.e., for 352 post-stimulus histograms. The histogram of distribution of standard deviation values derived from moving edges (marked as "σ_m") for both preferred directions for all cells examined is presented in Fig. 3(e). The σ-values varied from 0.4° to 3.3° with mean value of $1.5 \pm 0.5°$. In Fig. 3(d), these σ-values are plotted against RRF widths, estimated in the same units by means of maximum likelihood method. These two parameters appeared to be highly correlated (correlation coefficient was equal to 0.86). A slope of the best linear fit of the plotted data (solid line) determined the coefficient of proportionality. In order to estimate RRF width, σ-values of the best Gaussian fits should be multiplied by the coefficient $a = 3.3$.

3.2.2. *The Gaussian model of the RRF derived from flashing stripes*

Since OSUs respond to adequately oriented stationary light and dark stripes flashing at different positions of the stimulation area, RRF mapping can be addressed by means of such stationary stripes. In the experiment, stimuli were switched on sequentially in different parts of the stimulation area in quasi-random order. Stimulation was always initiated in the central part of the stimulation area. At the end of the procedure, stimulation was repeated in the central position in order to check

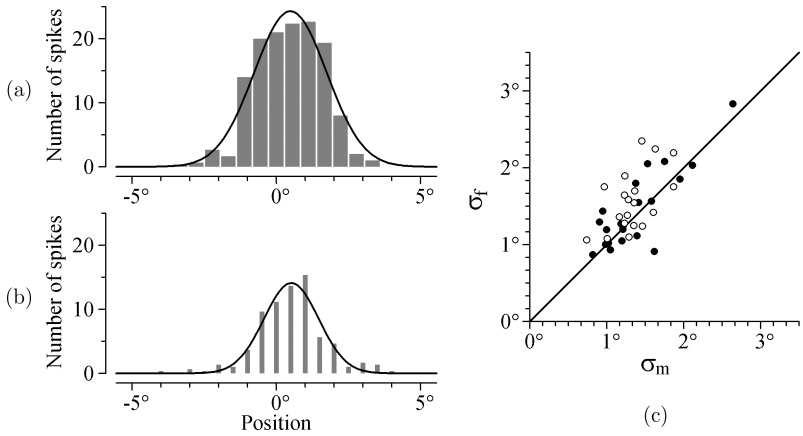

Fig. 4. Determination of parameters of the Gaussian model of the RRF from the OSUs responses to flashing stripes of preferred orientation. (a) Responses of the detector of horizontal lines to adequately oriented light flashing stripes of the width of $30'$; stimuli flashed on and off sequentially in different places of stimulation area in quasi-random order. Histogram represents distribution of number of spikes recorded at different positions of stimulation area; solid bell-shaped curve represent Gaussian approximation of cell responses at different positions of stimulation area. (b) Responses of the same detector of horizontal lines to adequately oriented light flashing stripes of the width of $10'$. Display format as in Fig. 3(a). (c) Scatter plot of the σ-values estimated by means of stationary flashing stripes (σ_f) versus the σ-values estimated by means of moving contrast edges (σ_m) pooled across different stimulus conditions for 38 OSUs. Open circles: data obtained for light stimuli; closed circles: data obtained for dark stimuli.

unit response level. Stimuli varied in width in different experiments from $10'$ to $1.1°$. Number of spikes was counted during the 500 ms from the onset of stimulation.

Results of the experiment made on a detector of horizontal line are shown in Figs. 4(a) and 4(b). Histograms of calculated number of spikes at different positions of the stimulation area are presented in Figs. 4(a) and 4(b). Results were obtained for light flashing stripes of different widths: $30'$ and $10'$ for Figs. 4(a) and 4(b), respectively. The widths of histogram bars correspond to the widths of the stimuli. Distributions of spike number were approximated by Gaussian curves (2.2). Both Gaussian fits were centered in the same position. Irrespective of the width of stimuli, the RRF size estimated by the Gaussian model was approximately $3°$ for this unit.

In the case of rather narrow stripes, one could expect the magnitude of the cell response to be proportional to the width of stripes. However, as one can see from the Figs. 4(a) and 4(b), the response amplitudes were not proportional to the stimulus width. The stimuli which was three times wider evoked responses of only 1.7 times higher amplitude. Absence of linear summation of signals from spatially separated regions within the center could be a consequence of inhibitory influences and/or nonlinear transformation of signals in the RRF.

In order to compare results derived by means of moving edges (σ_m) and flashing stripes (σ_f), σ-values, obtained by these two sets of stimuli in the same OSUs, were plotted against each other in Fig. 4(c). Data obtained by light (18 cells) and

dark stimuli (20 cells) are represented by open and closed circles, respectively. The data obtained for dark stimuli did not significantly differ from each other — corresponding points lie on the bisector of the coordinate angle. Some excess (also statistically insignificant) of the width of the RRF, obtained in measurement with the light flashing stripes, can be attributed to scattered light, which is inevitable in the application of bright light stimuli [6, 11].

3.3. *The difference of Gaussians models of the OSU RF*

Classical concentric RFs have an excitatory central part, which are surrounded by inhibitory periphery [11,22]. Their one-dimensional analogue — the simple receptive fields of the cat visual cortex [14] — consists of a narrow central excitatory zone flanked on both sides by inhibitory fields. It was natural to expect that the OSUs projecting to the fish tectum also possess similar inhibitory surround. Experimental procedures described in Secs. 3.1 and 3.2 gave us the information about width and form of the excitatory center of the OSU RF. However, due to lack of spontaneous activity it was not possible to investigate inhibitory influences by means of these procedures. Absence of cell response to adequately oriented stimuli presented in certain area may be caused by inhibitory inputs from the stimulated area, as well as by absence of any connection between explored cell and the stimulated area. In order to determine influence of the surround to responses evoked in the RF of the fish OSUs, two special experimental procedures were applied in the present study.

3.3.1. *Mapping the RF by two flashing stripes*

The first method uses some reference stimulus, which evoked certain excitation in the cell. This excitation can be increased or reduced by the influence of the test stimuli presented to the other locations within the RF. Then the decrease of the response in the simultaneous presentation of these stimuli could be interpreted as an inhibitory effect. In this method the reference stimulus was a stripe flashed in the center of the RF, while the test stripe flashed in different parts of the stimulation area in a quasi-random order. At the beginning of the experiment only the central stripe was stimulated by flashing. Number of spikes evoked by each flash of the test stimulus was counted. After presentation of the reference stimulus, we started to investigate how stimulation of neighboring locations of the visual field influenced the reaction in response to stimulation of the central stripe, which was made by stimulation with two flashing stripes. The influence of the test stripe on the central one was determined by the difference between mean number of spikes in response to stimulation of two stripes and mean number of spikes in response to reference stimulus alone. When this value was negative, one could say that there was an inhibitory influence from the second stimulus. The responses to two stripes were mapped considering the position of the second flickering stimulus.

Unfortunately, this method had one disadvantage. During the procedure a central part of the RRF was exposed to repeated stimulation by the reference stimulus.

The OSUs accustomed to the repeated stimulation and the number of spikes in the cell response progressively decreased by the end of the procedure; whereas the amplitude of spikes remained constant (which is an indicator of stability of the recording). Therefore, for investigation of surround effects, only those OSUs were selected, which did not exhibit marked adaptation to repeated stimulation.

In Fig. 5 results obtained for two detectors of horizontal lines by means of two experimental procedures: stimulation by one flashing stripe (see Sec. 3.2.2), and stimulation by two simultaneously flashing stripes, are compared. The detector of horizontal lines represented in Fig. 5(a) was stimulated by light stripes, while the one shown in Fig. 5(b) was excited by dark stripes; stimulus widths were 17′ and 23′, respectively. Widths of histogram bars in the figure corresponded to the widths of stimuli. Histograms showing distributions of spike number along the RRF area in two mentioned OSUs, obtained by means of stimulation with one flashing stripe are represented in the top diagrams. Results are approximated by corresponding Gaussian profiles and are shown with solid bell-shaped curves. Bottom histograms in Figs. 5(a) and 5(b) show results obtained by means of stimulation of the same cells by two stripes that flashed simultaneously. Black thin horizontal lines on the

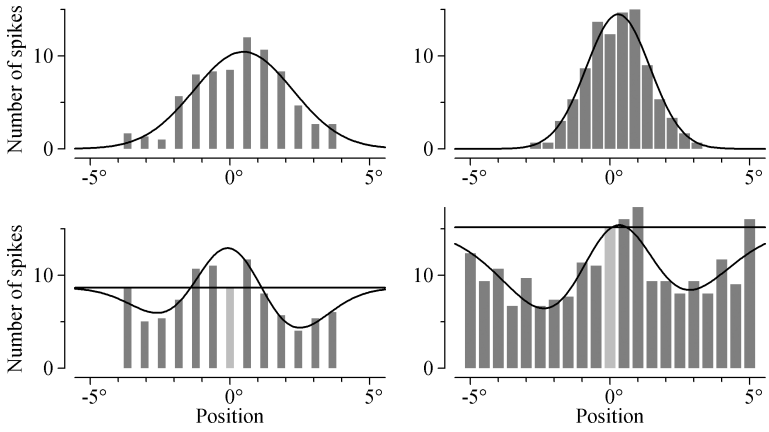

(a) (b)

Fig. 5. Histograms showing distribution of spike discharges across stimulation area recorded in two detectors of horizontal lines by means of two experimental procedures: stimulation by one adequately oriented flashing stripe at different parts of stimulation area (top histograms) and stimulation by two simultaneously flashing stripes of preferred orientation (bottom histograms). The number of spikes recorded during 500 ms after onset of the stimulus served as a measure of the magnitude of the cell response. The data on the top histograms are approximated by the Gaussian curves (solid bell-shaped curves), while the data on bottom histograms are fitted by DoG-profiles (solid DoG-curves). Thin horizontal lines on the bottom histograms represent amplitude levels of the responses to reference stimuli. The responses to two stripes were mapped considering the position of the second flashing stimulus. (a) Detector of horizontal lines stimulated by light flashing stripes; stimulus width 17′; widths of histogram bars correspond to the widths of stimuli. (b) Detector of horizontal lines stimulated by dark flashing stripes; stimulus width 23′; widths of histogram bars correspond to the widths of stimuli.

histograms represent amplitude levels of the responses to reference stimuli, placed in the center of the stimulation area. These results are approximated by DoG-function (2.3) shown with solid curves at the bottom diagrams of Figs. 5(a) and 5(b).

A total of 92 OSUs were studied by the method of two flashing stripes. In all cases, we observed an inhibitory effect of the surround. This inhibition had the following properties: (1) the inhibitory zone noticeably extended beyond the RRF area, as shown in Fig. 5(b), and (2) the zone of inhibition always started inside the RRF area, so that an excitatory central zone of the RF was always distinctly narrower than the RRF determined by using flashing stripes. However, the value of inhibition and position of the boundary at transition from central excitatory zone to inhibitory surround greatly changed with the conditions of stimulation. Therefore, attempts to describe uniformly the structure of the RF using linear difference of Gaussians model did not give satisfactory results.

In all responses from two simultaneously flashing stripes it can be seen that they did not sum linearly even inside the RF center (see also Fig. 5). Responses from the two stripes were always seen to be smaller in amplitude than the sum of the responses evoked by each of the stripes separately (compare DoG and Gaussian profiles in Fig. 5). In some cases, maximal recorded response from two stripes was seen to be of the same amplitude as the response to reference stimulus alone. Indeed, in the cell shown in Fig. 5(b), response to central stimulus was inhibited by practically all peripheral stripes. Thus, stimulation by two flashing stripes revealed surround suppression in the OSU RF. Inhibitory influences of the second (peripheral) stimulus were recorded at a certain distance from the central stripe in all cells examined. These inhibitory influences, estimated by the DoG-profiles, were seen to always initiate inside the RRF area and move away from the RRF.

3.3.2. *Center/surround antagonism derived from flashing stripes of different width*

Another experimental method (besides the stimulation by two stripes) that revealed the presence of the surround suppression consisted of stimulation by stripes of different widths, and a subsequent analysis of the relationship between cell response and the width of the stimulus. Within the framework of the linear model of the RF consisting of excitatory center and inhibitory surround (an example of which is the difference of the Gaussians model), the dependence of the cell response on the stripe width is as follows: at first the response magnitude increases with an increase in the width of the stripe centered on the RF until its size becomes as large as the excitatory area of the RF, and then the response magnitude decreases as the stimulus becomes larger and activates the inhibitory surround. This provides an experimental procedure for measurement of the width of the excitatory center of the RF as the width of stripe, at which the magnitude of the response reaches its maximum.

In experiments, inhibitory influences in the OSU RF were evaluated by means of appropriately oriented flashing stripes with varying width during the procedure.

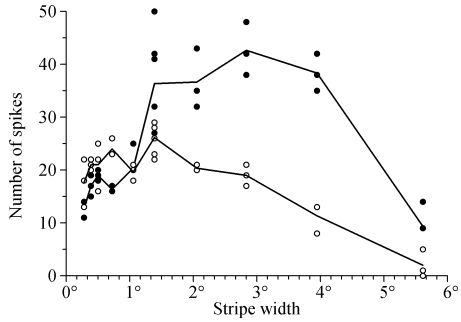

Fig. 6. Amplitudes of responses recorded in a detector of horizontal lines to stimulation by light and dark stripes of different widths. Three stimulus trials were repeated over each stimulus width. Open and closed circles represent response amplitudes, recorded for light and dark stripes, respectively. Mean amplitudes of responses at different stimulus widths are joined by the solid lines.

Stripes of different widths were presented in the RF center sequentially in quasi-random order. Three stimulus trials were repeated over each stimulus width. Figure 6 shows a typical result. In all investigated cells, magnitude of responses reached a maximum at a certain width of stripe, and then began to decrease. From the example shown in Fig. 6 one can see that the responses to either light or dark stimuli started to decrease at a certain stimulus width. However, the responses to light and dark stripes reach their maximum values at significantly different values. In the framework of the linear model of the interaction of an excitatory center and inhibitory surround, this means that the size of the excitatory center was substantially different for light and dark stimuli. This feature was observed in all 16 OSUs tested by this method. It is the most striking manifestation of violation of the symmetry of ON and OFF properties of the OSUs. For the cell shown in Fig. 6, the width of the RRF was measured in an independent experiment, using flashing narrow light stripes. It turned out to be equal to $3°30'$. That exceeds estimates of width of the excitatory center for both dark and light stripes obtained here. It should also be noted that in most units maximal response amplitudes recorded for dark stripes were significantly higher than for light ones (see Fig. 6). Thus, one can expect that the ON and OFF channels process signals in different ways in the fish retina.

4. Discussion

4.1. *Receptive field sizes of OSUs*

The comparison of OSU RRFs of different types had revealed that RRFs of detectors of vertical lines are significantly wider (13%) than those of detectors of horizontal lines. Such result seems to contradict our current knowledge about the organization of the receptive field sizes of orientation-selective units. In the work of Maximova and Maximov [32] it was shown that responses of both OSUs, one detector of vertical lines and one detector of horizontal lines, could be recorded simultaneously at each

point of the tectum (at one appropriate electrode position), their receptive fields almost coincided in their positions. Consequently, one may infer that detectors of vertical and horizontal lines are distributed over the retina with equal density. Next, it is known that ganglion cells of each type form mosaics. Their dendrites tile the retina without overlapping [37,38]. Therefore, considering the equal retinal densities of two types of OSUs one can infer that the RRFs of both types of detectors have to be equal in area. Contradiction of this statement from the results of the present study can be explained. We measured the RRF sizes along only one direction, orthogonal to the preferred edge orientation, i.e., for detectors of vertical lines we measured only the horizontal widths of the RRFs and for detectors of horizontal lines we measured only the vertical widths of the RRFs. At the same time other types of fish ganglion cells were shown to possess receptive fields of ellipsoidal shapes, elongated predominantly in the horizontal direction. Receptive fields of the great majority of *C. gibelio* direction-selective ganglion cells happened to be elongated horizontally. The mean aspect ratio between the minor and major axes of their RRFs, calculated for $n = 99$ cells was 0.8 ± 0.11 [7]. We did not estimate RRF shapes of other fish movement detectors systematically. However, our pilot observations of spot detectors indicated that their RRFs were also ellipsoidal in shape and elongated horizontally. Thus, we hypothesize that the visual system of fish is anisotropic, and its vertical resolving ability is higher than the horizontal one due to the elongation of the ganglion cells RRFs in the horizontal plane.

Statistically significant difference was also revealed between sizes of the RRFs evaluated by moving light and dark edges (the stimuli with different signs of contrast). The mean RRF width, estimated for leading light edges (ON responses) were significantly wider than those evaluated for leading dark edges (OFF responses). Due to the ON–OFF nature of OSUs, one can suppose that dendrites of orientation-selective ganglion cells branch in ON and OFF sublaminae of the inner plexiform layer. Similar pattern is known for the mammalian fast ON–OFF direction-selective ganglion cells, where they are bistratified, their ON and OFF dendritic arbors branching in different sublaminae of the inner plexiform layer of the retina [1,21,39]. Sizes of the RRFs of ganglion cells are considered to be determined by the areas covered by dendritic arbors, and so one can look for an explanation of the different widths of RRF for ON and OFF responses, observed in the present study, in difference in sizes of dendritic branches in ON and OFF sublaminae of the inner plexiform layer. However, the sizes of dendritic arbors of same cells in different sublaminae should not differ, since they form mosaics and tile without overlapping. Therefore, the difference in the size of the RRF of ON and OFF channels found here requires a different explanation.

RRFs of different types of detectors were studied in the tectal retinorecipient layer of *C. gibelio* [7, 29, 30]. Results of previous work, along with results of the present study gave support for laminar and columnar architecture of fish retinotectal projections. First, it was shown that RRFs of different types of detectors,

recorded in different sublaminae of retinorecipient layer during the perpendicular track of electrode through the tectum, appeared to be centered in approximately the same position. Second, RRFs of *C. gibelio* OSUs, estimated in the present study, were shown to be of approximately the same size as RRFs of direction-selective units evaluated recently in the same species [7]. Practically identical widths and positions of RRFs, recorded in different types of detectors along columns of tectal retinorecipient layer, indicate that elementary parts of visual scene (about 4.5–5° in diameter) are analyzed by different types of fish movement detectors. Laminar-specified circuits from retina to midbrain were described in other vertebrate species. Laminar architecture of retino-tectal projections described in chicken reveals four retinorecipient sublaminae in the retinorecipient layer [40]. Laminar architecture of retinal projections to midbrain was described in mammals as well. Laminar and columnar specificity of retinal projections to mouse superior colliculus were described in a recent work [16]. Thus, one can say that retino-tectal projections in fish are specified by laminar and columnar architecture, analogous to structures in midbrains of other vertebrates.

4.2. *Receptive field structure of OSUs*

Failure of a simple linear "integrate-and-fire" model (where the cell response was determined by sum of all inputs with some weights) were seen in experiment of the RRF mapping by stationary stripes or in experiment with stimulation by two stripes of preferred orientation that flashed simultaneously. In both cases, there was a lack of activity of signals from spatially separated regions even within the excitatory RRF center. Another inconsistency occurred when comparing the results of different experiments on the center/surround antagonism conducted on the same unit. In the case of linear summation, RF profile as a DoG-function can be obtained by approximation of the results of experiments in which stimulation by two simultaneously flashing narrow stripes were used (Sec. 3.3.1). Amplitude of responses of the unit to stripes of various widths can be predicted by the integration of this DoG-function within corresponding limits. This prediction can then be compared with results of a direct experiment on measurement of the relationship between cell response and the width of the stimulus (Sec. 3.3.2).

An example of such a comparison, conducted for the same detector of horizontal line that is shown in Fig. 5(a), is presented in Fig. 7. As described in Sec. 3.3.1, the unit was stimulated by two narrow (17′) light stripes, one of which was always placed in the center of the stimulation area, while the other was located at different places on each side. The number of spikes was recorded at 500 ms after onset of the stimuli. The result was approximated by the DoG-function, which is shown by the continuous curve in insets to the right in Fig. 7. Integration of this function in the interval of $(-d/2, +d/2)$ predicted the amplitude of a response of the same cell to a centered light stripe of width d, assuming that all other parameters of stimulation and recording (the stripe and background brightness, time of presentation,

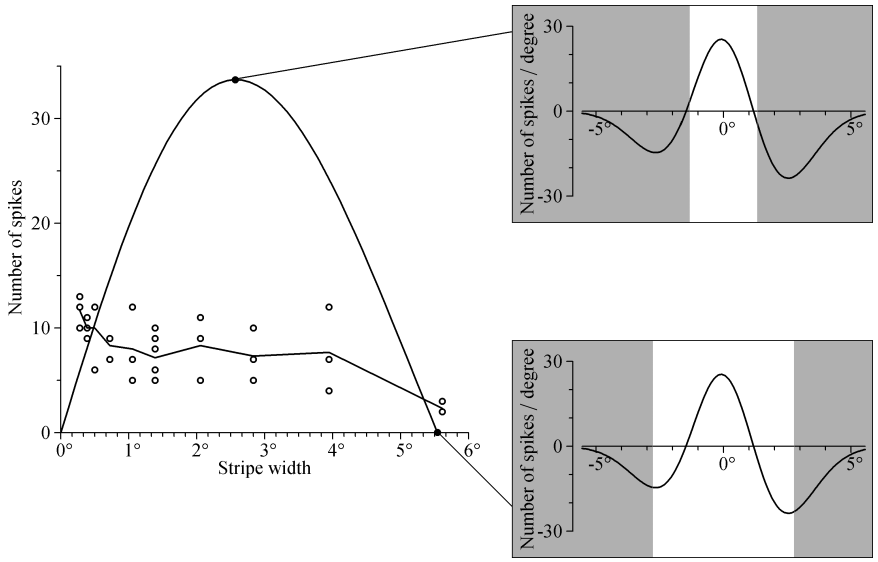

Fig. 7. Diagram representing dependence of the cell response on the stimulus width (see text for detailed explanation).

etc.) were the same. The resulting relationship between the predicted response and the width of the stripe is shown by a smooth curve in Fig. 7. Insets to the right show positions of the light stripe within the RF for the two particular points of the curve. The upper inset corresponds to the stripe which width is equal to the width of the excitatory center of the RF. With this width the curve reaches its maximum. The lower inset corresponds to the stripe that covers such a portion of the inhibitory surround, which exactly compensates the excitation of the central zone. The cell should not respond to the stripe of such width. Open circles in the diagram show the results of a direct measurement of dependence of amplitude of the cell response on the width of the light stripes for the same unit. Three stimulus trials were repeated over each stimulus width. Mean amplitudes of responses at different stimulus widths are joined by a solid line. One can see that amplitudes of responses to flashing stripes of different widths, predicted by the integrated DoG curve are underestimated by experimental results. This fact suggests that responses to stimuli of different widths are not linearly summed inside OSU RRF. Absence of linear signal summation across RRF indicates that OSU RRF cannot be defined by a homogeneous sensory zone driven by a linear mechanism of response generation.

Extracellular recordings from tectal projections of fish OSUs in the present study gives strong evidence for inhibitory influences in the fish OSU RF. In experiments with stimulation by two stripes of preferred orientation that flashed simultaneously, the inhibitory influences of the second (peripheral) stimulus was always initiated inside the RRF area. This property of the lateral inhibition, together with nonlinear summation within the RF, suggests that the OSU RF in fish appears to be functionally divided into subunits sensitive to the appropriately oriented stimuli, and

that the RFs of subunits should be influenced by inhibition of the surround with subsequent nonlinear summation.

Acknowledgments

We are grateful to Paul Maximov for his engineering support of the experiments and Roman Poznanski for his valuable comments and suggestions for the manuscript. The study was supported by grant 07-04-00516 from the Russian Foundation for Basic Research.

References

[1] Amthor FR, Oyster CW, Takahashi ES, Morphology of on-off direction-selective ganglion cells in the rabbit retina, *Brain Res* **298**:187–190, 1984.

[2] Amthor FR, Takahashi ES, Oyster CW, Morphologies of rabbit retinal ganglion cells with complex receptive fields, *J Comp Neurol* **280**:97–121, 1989.

[3] Barlow HB, Hill RM, Levick WR, Retinal ganglion cells responding selectively to direction and speed of image motion in the rabbit, *J Physiol (Lond)* **173**:377–407, 1964.

[4] Bloomfield SA, Orientation-sensitive amacrine and ganglion cells in the rabbit retina, *J Neurophysiol* **71**:1672–1691, 1994.

[5] Bowling DB, Light responses of ganglion cells in the retina of the turtle, *J Physiol (Lond)* **299**:173–196, 1980.

[6] Cicerone CM, Green DG, Signal transmission from rods to ganglion cells in rat retina after bleaching a portion of the receptive field, *J Physiol (Lond)* **314**:213–224, 1981.

[7] Damjanović I, Maximova EM, Maximov VV, Receptive field sizes of direction-selective units in the fish tectum, *J Integr Neurosci* **8**:77–93, 2009.

[8] Devries SH, Baylor DA, Mosaic arrangement of ganglion cell receptive fields in rabbit retina, *J Neurophysiol* **78**:2048–2060, 1997.

[9] Gesteland RC, Howland B, Lettvin JY, Pitts WH, Comments on microelectrodes, *Proc IRE* **47**:1856–1862, 1959.

[10] Girman SV, Sauve Y, Lund RD, Receptive field properties of single neurons in rat primary visual cortex, *J Neurophysiol* **82**:301–311, 1999.

[11] Hartline HK, The receptive fields of optic nerve fibers, *Am J Physiol* **130**:690–699, 1940.

[12] He S, Levick WR, Vaney DI, Distinguishing direction selectivity from orientation selectivity in the rabbit retina, *Visual Neurosci* **15**:439–447, 1998.

[13] Hubel D, *Eye, Brain and Vision*, Scientific American Library, New York, 1988.

[14] Hubel D, Wiesel T, Receptive fields, binocular interactions and functional architecture in cat's visual cortex, *J Physiol (Lond)* **160**:106–154, 1962.

[15] Hubel D, Wiesel T, Receptive fields and functional architecture of monkey striate cortex, *J Physiol (Lond)* **195**:215–243, 1968.

[16] Huberman AD, Manu M, Koch SM, Susman MW, Lutz AB, Ullian EM, Baccus SA, Barres BA, Architecture and activity-mediated refinement of axonal projections

from a mosaic of genetically identified retinal ganglion cells, *Neuron* **59**:425–438, 2008.

[17] Ibbotson MR, Price NSC, Crowder NA, On the division of cortical cells into simple and complex types: A comparative viewpoint, *J Neurophysiol* **93**:3699–3702, 2005.

[18] Jacobson M, Gaze RM, Types of visual response from single units in the optic tectum and optic nerve of the goldfish, *Q J Exp Physiol* **49**:199–209, 1964.

[19] Kagan I, Gur M, Snodderly DM, Spatial organization of receptive fields of V1 neurons of alert monkeys: Comparison with responses to gratings, *J Neurophysiol* **88**:2557–2574, 2002.

[20] Kawasaki M, Aoki K, Visual responses recorded from the optic tectum of the Japanese dace, *Tribolodon hakonensis, J Comp Physiol A* **152**:147–153, 1983.

[21] Kittila CA, Massey SC, Pharmacology of directionally selective ganglion cells in the rabbit retina, *J Neurophysiol* **77**:675–689, 1997.

[22] Kuffler SW, Discharge patterns and functional organization of the mammalian retina, *J Neurophysiol* **16**:37–68, 1953.

[23] Lettvin JY, Maturana HR, McCulloch WS, Pitts WH, What frog's eye tells to the frog's brain, *Proc Inst Radio Engrs NY* **47**:1940–1951, 1959.

[24] Leventhal AG, Schall JD, Structural basis of orientation sensitivity of cat retinal ganglion cells, *J Comp Neurol* **220**:465–475, 1983.

[25] Liege B, Galand G, Types of single-unit visual responses in the trout's optic tectum, in Gidikov A (ed.), *Visual Information Processing and Control of Motor Activity*, Bulgarian Academy of Sciences, Sofia, pp. 63–65, 1971.

[26] Maturana HR, Frenk S, Directional movement and horizontal edge detectors in the pigeon retina, *Science* **142**:977–979, 1963.

[27] Maturana HR, Lettvin JY, McCulloch WS, Pitts WH, Anatomy and physiology of vision in the frog, *J Gen Physiol* **43**:129–175, 1960.

[28] Maximov VV, Maximova EM, Maximov PV, Direction selectivity in the goldfish tectum revisited, *Ann NY Acad Sci* **1048**:198–205, 2005a.

[29] Maximov VV, Maximova EM, Maximov PV, Classification of direction-selective units recorded in the goldfish tectum, *Sensory Systems* **19**:322–335, 2005b (in Russian).

[30] Maximov VV, Maximova EM, Maximov PV, Classification of orientation-selective units recorded in the goldfish tectum, *Sensory Systems* **23**:13–23, 2009 (in Russian).

[31] Maximova EM, Colour and spatial properties of detectors of oriented lines in the fish retina, *Iugoslav Physiol Pharmacol Acta* **34**:351–357, 1998.

[32] Maximova EM, Maximov VV, Detectors of the oriented lines in the visual system of the fish *Carassius carassius*, *J Evol Biochem Physiol* **17**:519–525, 1981 (in Russian).

[33] Maximova EM, Orlov OYu, Dimentnman AM, Investigation of visual system of some marine fishes, *Voprocy Ichtiologii* **1**:893–899, 1971 (in Russian).

[34] Mechler F, Ringach DL, On the classification of simple and complex cells, *Vision Res* **42**:1017–1033, 2002.

[35] Michael CR, Color-sensitive complex cells in monkey striate cortex, *J Neurophysiol* **41**: 1250–1266, 1978.

[36] Rodieck RW, Stone J, Analysis of receptive fields of cat retinal ganglion cells, *J Neurophysiol* **28**:832–849, 1965.

[37] Rockhill RL, Daly FJ, MacNeil MA, Brown SP, Masland RH, The diversity of ganglion cells in a mammalian retina, *J Neurosci* **22**:3831–3843, 2002.

[38] Wässle H, Peichl L, Boycott BB, Morphology and topography of on- and off-alpha cells in the cat retina, *Proc R Soc Lond B* **212**:157–175, 1981.

[39] Weng S, Sun W, He S, Identification of ON-OFF direction-selective ganglion cells in the mouse retina, *J Physiol (Lond)* **562**:915–923, 2005.

[40] Yamagata M, Weiner JA, Dulac C, Roth KA, Sanes JR, Labeled lines in the retinotectal system: Markers for retinorecipient sublaminae and the retinal ganglion cell subsets that innervate them, *Moll Cell Neurosci* **33**:296–310, 2006.

[41] Zenkin GM, Pigarev IN, Detector properties of the ganglion cells of the pike retina, *Biophysics* **14**:722–730, 1969 (in Russian).